The 7th International Conference of Asian Concrete Federation
"SUSTAINABLE CONCRETE FOR NOW AND THE FUTURE"
30 Oct – 02 Nov, 2016, Hanoi, Vietnam
www.acf2016.vn

INFLUENCE OF PLACING METHOD CONSIDERING FIBER ORIENTATION TO BENDING CHARACTERISTICS OF DFRCC

K. Watanabe[1], Y. Ozu[1], M. Miyaguchi[2], and T. Kanakubo[3]

[1] *Master Program, Dept. of Engineering Mechanics and Energy, University of Tsukuba, Tsukuba, Japan*
[2] *Sumitomo Mitsui Construction Co.,Ltd., Tokyo, Japan*
[3] *Professor, Dept. of Engineering Mechanics and Energy, University of Tsukuba, Tsukuba, Japan*

ABSTRACT: Ductile fiber-reinforced cementitious composites (DFRCC) are cementitious materials reinforced with short fibers to improve the tensile and bending ductility of mortar or concrete. It is well known that bending characteristics of DFRCC are influenced by fiber orientation. Controlling the fiber orientation is one of the effective methodology to make DFRCC more practical. In this study, placing methods considering fiber orientation using a vibrator and a device like a "comb" are newly proposed. Beam specimens of which cross-sectional size is 180×280mm are manufactured using DFRCC reinforced with polyvinyl alcohol (PVA) fiber. The parameter is placing method of DFRCC. Four-point bending test is carried out for these specimens. From the test result, the bending capacity and ductility increase in specimens applied moving a comb and a vibrator axial direction. It is confirmed that the fiber orientation tends to differ in each specimen and in positions of a cross-section by observing the specimen section after loading. The bending capacity of each specimen is evaluated by section analysis using the bridging law which expresses the difference of fiber orientation for the position of cross-section of the specimen.

1 INTRODUCTION

Ductile fiber-reinforced cementitious composites (DFRCC) are cementitious materials with mixing fiber in mortar or concrete. DFRCC shows multiple cracks and deflection hardening behavior under the bending stress filed. DFRCC is expected as one of the new cementitious materials which show high ductility for bending, tension, and compression behaviors those are improved largely than ordinary concrete. It is known that the characteristics of fiber-reinforced cementitious composites are affected by the distribution and orientation of fiber in matrix. To apply DFRCC for practical use, controlling of fiber orientation is important to improve and stabilize the characteristics of DFRCC. In this study, placing methods considering fiber orientation using a vibrator and a device like a "comb" are newly proposed. Beam specimens of which sectional size is 180×280mm are manufactured using DFRCC reinforced with polyvinyl alcohol (PVA) fiber. Four-point bending test is carried out for these specimens. The flow analysis using a wide-use software based on finite-difference method (FDM) is also conducted to simulate the flow of matrix and fiber orientation. The bending capacity of each specimen is evaluated by section analysis considering the difference of fiber orientation in the cross-section of the specimen.

2 OUTLINE OF PLACING METHOD

Placing methods of DFRCC proposed in this study are shown in Figure 1. While the normal placing (N) means that the DFRCC filled into the mold only by flow (self-compacting), the comb device is applied (CA) to arrange the fiber orientation longitudinally. A vibrator is applied with moving in the mold for axial direction (VA) and perpendicular direction (VP).

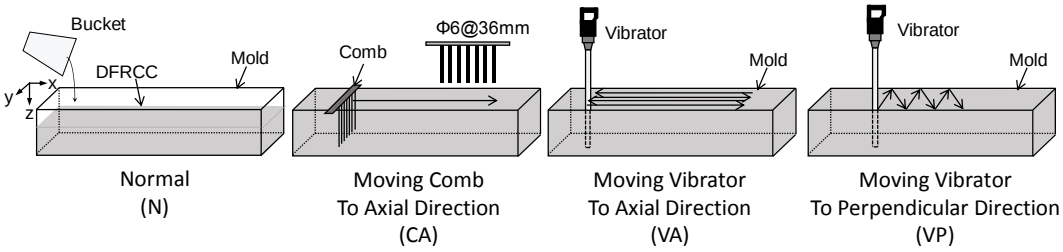

Figure 1. Proposed placing method

3 BENDING TEST

3.1 Material properties

The mix proportion of DFRCC is shown in Table 1. Polyvinyl alcohol (PVA) fiber which length is 12mm, diameter is 0.10mm is used. The fiber volume fraction is 2.0%. Fresh and mechanical property of DFRCC are shown in Table 2. After sealed curing for 8 days, the specimens were cured in atmospheric environments. The testing age at bending test ranges 29 – 31 days.

Table 1. Mix proportion of DFRCC (kg/m^3)

Water	Cement	Fine aggregate	Fly ash	PVA fiber	High performance water reducing agent	Thickening agent
380	678	484	291	26	6	2.52-3.03

Table 2. Fresh and mechanical property of DFRCC

Air content (%)	Compressive strength (MPa)	Elastic modulus (GPa)
1.8	45.6	13.9

3.2 Loading and measurements

Outline of four-point bending test is shown in Figure 2. The displacement controlled 2MN universal testing machine was used. The loading speed was set to 0.5mm/min. The measuring items were applied load, the displacements at loading points (2 points) and local deformation to calculate the crack width and curvature. After loading, number of cracks generated in pure bending section was counted visually.

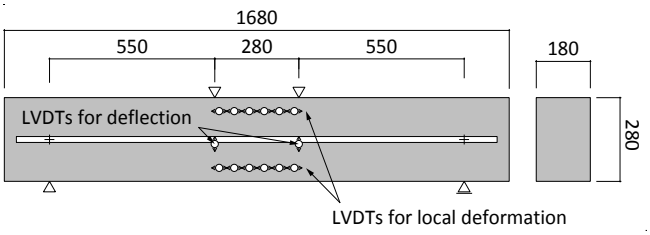

Figure 2. Specimen

4 EXPRIMENTAL RESULT

4.1 Placing observation

Figure 3 shows the example of photos in placing for the specimen N and CA. During self-compacting, DFRCC matrix are spreading in concentric circles around the placing point. Near the vertical mold walls, DFRCC matrix are flowing along the walls. When the comb device moved, tracks of the comb device are observed. In specimens VA and VP, tracks due to moving a vibrator are also observed.

Figure 3. Placing and moving a comb device

4.2 Bending moment-deflection curve

Bending moment – deflection curves are shown in Figure 4, the test results are summarized in Table 3. Deflection is obtained as the average of two LVDTs at the loading points. The bending capacity and ductility of specimens CA and VA are larger than those of specimen N. It is considered that fibers are arranged toward the longitudinal direction as the result of moving the vibrator and the comb, and resistance performance to crack opening increases. While bending capacity of specimen VP is similar as that of specimen N, ductility is larger than specimen N.

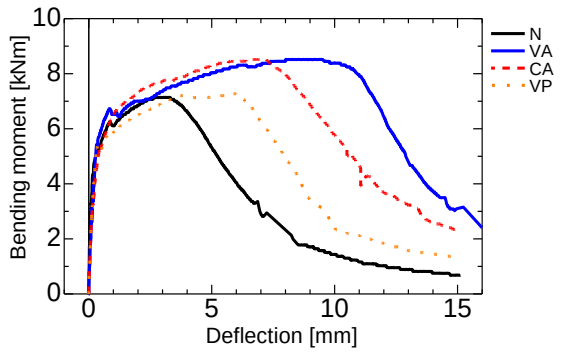

Figure 4. Bending moment – deflection curve

Table 3. Bending test results

Specimen	At maximum load		
	Max. Load (kN)	Deflection (mm)	Bending moment (kNm)
N	26.0	3.04	7.14
VA	31.0	8.13	8.52
CA	31.0	6.63	8.53
VP	26.5	5.85	7.28

4.3 Crack pattern observation

The crack patterns after loading are shown in Figure 5. The number of cracks generated in pure bending section is listed in Table 4. The cracks at the tension zone of 42mm (specimen depth 280mm×0.15) from the bottom were counted. In all specimens, after four or five cracks taking place, one of them is mainly

opened. The average crack spacing is calculated as pure bending span 280mm divided by the number of cracks in each specimen.

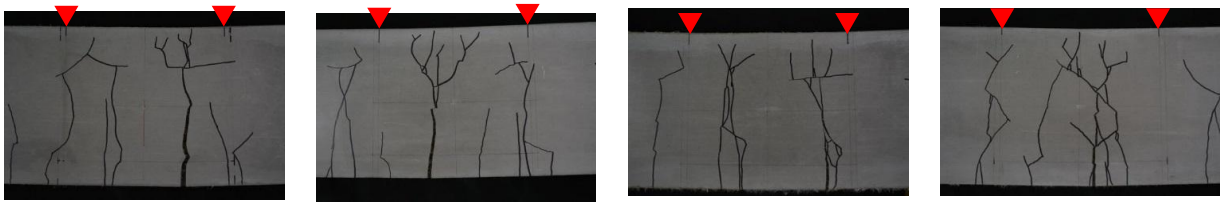

N VA CA VP

Figure 5. Crack patterns after loading (triangles show loading points)

Table 4. Number of cracks and average crack spacing

Specimen	Number of cracks	Average crack spacing (mm)
N	4	70
VA	5	56
CA	5	56
VP	4	70

4.4 Fracture surface observation

Specimen was ruptured into two pieces after loading at the major crack, and the fracture surface was observed visually. The photos of fracture surfaces are shown in Figure 6. The black-light was used for easiness of visual observation. The dotted straight lines in the figure indicate the mold surfaces. The matrix was poured from the upper surface in the photos. In specimen N, while fibers near the mold tend to be along the mold surface, fibers at the central section tend to be arranged toward the perpendicular direction for specimen axis (shown by arrows). Fibers in specimen VP are observed like swirling. In specimens CA and VA, fibers have tendency to be rearranged to longitudinal direction. It is observed that fibers in the center of section orient more axial direction of specimen. As the result of the surface observation, fiber orientation can be controlled by the moving vibrator and comb longitudinally.

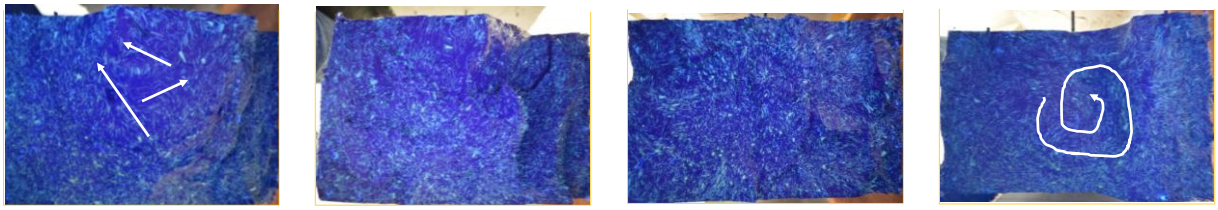

N VA CA VP

Figure 6. Fracture surfaces observation

5 FLOW ANALYSIS

5.1 Simulation method

The flow analysis is conducted using a general-purpose computational fluid dynamics (CFD) software based on finite-difference method (FDM) by controlling volume (FLOW-3D). The fibers are replaced by the unit vector in each calculated mesh, the vector is obtained as the results of fluid flow calculation which is given by the coordinates of x, y and z of direction vector. So, collisions of fibers and influence of flow of fibers themselves cannot be considered. The difference of fiber volume fraction also cannot be taken account. Analysis conditions are listed in Table 5. To simulate the actual DFRCC placing carried out in manufacturing the bending specimens, a flow-out hole was considered in the analysis. The position of

the flow-out hole is shown in Figure 7. Fluid density was set to be the same as DFRCC, and fluid viscosity was decided from the flow test result of DFRCC as similar as described in the previous study (Kanakubo et al.(2016)). The radius of flow-out hole and the flow speed was decided to show the same filling time in manufacturing the bending specimen. The position of the hole is set as same as the actual DFRCC placing.

Table 5. Analysis conditions

Parameter	Input value	Parameter	Input value
Fluid viscosity (Pa*s)	4.36	Radius of flow-out hole *R* (mm)	12
Fluid density (g/cm^3)	1.96	Height of flow-out hole *h* (mm)	40
Flow time (s)	240	Position of flow-out hole *d* (mm)	250
		Flow speed *V* (mm/s)	78

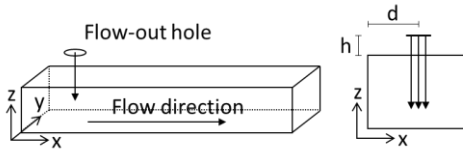

Figure 7. Position of flow-out hole

5.2 Result of flow analysis

Figure 8 and 9 shows the analysis results for xy plane and zx plane, respectively. The results for xy plane (Figure 8) show the phenomenon that fluid spread in concentric circles around the placing point like actual DFRCC pouring. As far from the placing point, fibers tend to orient randomly in the center of the mold. After finishing placing (t=240s), many fibers which lie perpendicularly are observed from enlarged view (right figure). From the results for zx plane (figure 9), fibers tend to orient along parabolic curve around the placing point. It is assumed that fluid rebounds up from the bottom of the mold when fluid placed. Rebounding fibers flow to the pure bending section remaining those orientations. While fibers tend to orient perpendicularly around the upper surface due to fluid pouring, fibers orient longitudinally at the bottom section.

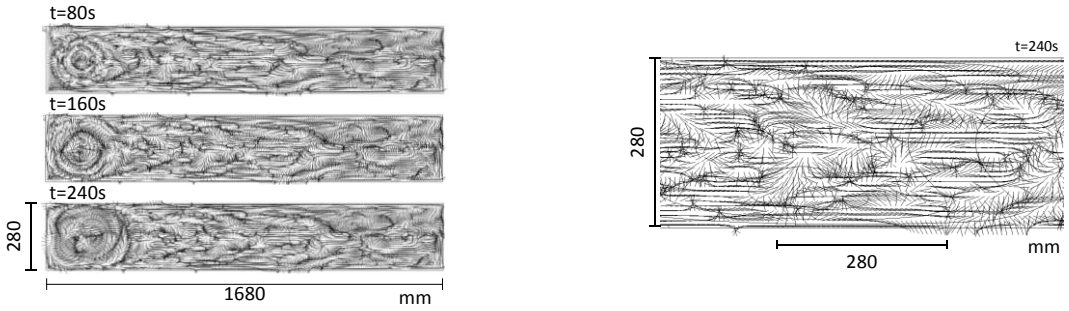

Figure 8. Analysis results for xy plane (right: enlarged view at 240s)

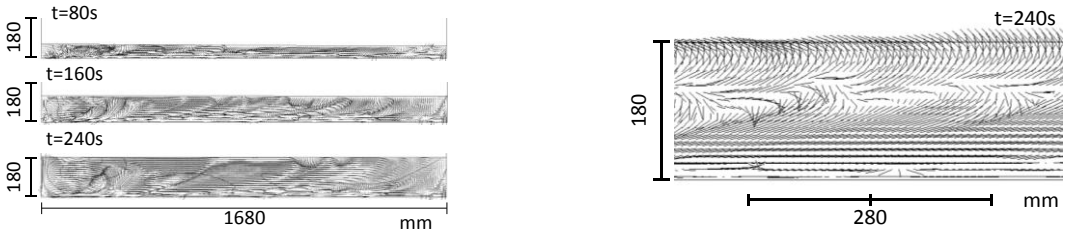

Figure 9. Analysis results for zx plane (right: enlarged view at 240s)

6 SECTION ANALYSIS CONSIDERING FIBER ORIENTATION

6.1 Model for DFRCC

It is confirmed that the fiber orientation tends to differ in each specimen and in positions of a cross-section by observing the fracture surface of the specimens after loading. To evaluate the bending capacity of each specimen, section analysis is conducted. The different bridging laws (tensile stress – crack width relationship) are applied to each position of divided 8 sections as shown in Figure 10. Employed relationships between the stress and the strain are shown in Figure 10. The parabolic model is adopted in the compression side, the trilinear model is adopted in the tension side. In the parabolic model, σ_B is 45.6 MPa, ε_c is 0.0046 from the compression test result of test pieces of DFRCC. The procedure of building up the trilinear model for tension side is shown in Figure 11. The bridging law is derived from the test result of pulling out of single PVA fiber considering the probability density function (PDF) which gives the fiber orientation distribution (Kanakubo et al.(2016)). The pullout model of single fiber is also shown in Figure 11. The values of P_a and P_{max} are assumed to be 1.5N and 3.0N, respectively. The values of δ_a and δ_{max} are set to 0.2mm and 0.45mm, respectively, as same as previous study (Kanakubo et al.(2016)). The elliptic function is adopted as the PDF for fiber orientation distribution (Kanakubo et al.(2016)). The orientation intensity, which is defined as the ratio of two radii, k(=a/b), and the principal orientation angle ϑ_r can indicate the intense of the fiber orientation tendency toward the principal orientation angle. In this study, ϑ_r is set to 0 (longitudinal direction). The fiber orientation is expressed by difference of the orientation intensity k. If k=1, it means fibers exist randomly. k>1 means that fibers tend to orient longitudinal direction, k<1 means fibers tend to orient to perpendicular direction. The input value for the parameters are listed in Table 6. The coefficients to show snubbing effect and the fiber strength degradation are set to 0.5 and 0.3, as same as those in the previous study (Kanda and Li (1999)). The rupture strength is 569MPa that is the average of rupture strength obtained in previous pullout test of single fiber (Asano (2014)). The bridging law is calculated as the summation of pullout load of fibers that exist on a crack surface. After that, the bridging law is modeled to trilinear model, which is characterized by two points corresponding to the maximum stress and the point to show remarkable changing of the slope. In order to use the bridging law in the section analysis, the crack width is converted to strain, namely, crack width is divided by the average crack spacing observed in the bending test (Table 4). The values for the first point (σ_{bs}, ε_{bs}) and the second point (σ_2, ε_2) are listed in Table 7.

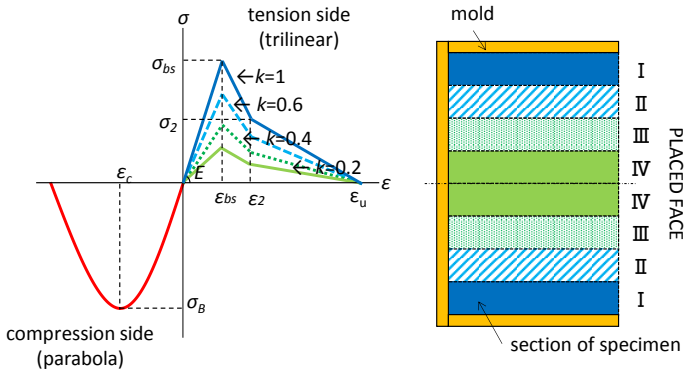

Figure 10. Relationship between stress versus strain and specimen section

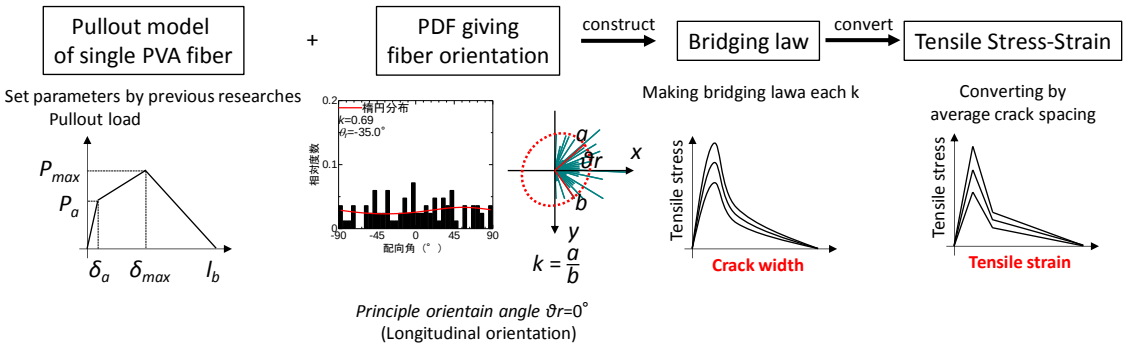

Figure 11. Procedure of building up the trilinear model for tension side

Table 6. Input values for bridging law

Parameter	Input value	Parameter	Input value
First peak load, P_a (N)	1.5	Fiber strength (MPa)	569
Crack width at P_a, δ_a (mm)	0.2	Snubbing coefficient, f	0.5
Maximum load, P_{max} (N)	3.0	Fiber strength reduction factor, f'	0.3
Crack width at P_{max}, δ_{max} (mm)	0.45		

Table 7. Characteristic values for trilinear model for tension side

k	σ_{bs}	ε_{bs}	σ_2	ε_2	ε_u
0.7	1.87	0.00325	0.45	0.0075	0.100
0.6	1.78	0.00300	0.39	0.0075	0.100
0.4	1.54	0.00300	0.27	0.0075	0.100
0.2	1.15	0.00300	0.14	0.0075	0.100

6.2 Result of section analysis

The different bridging laws are applied to each position of divided 8 sections of the specimen as shown in Figure 10. The orientation intensity is decided as the maximum bending moment measured in the bending test corresponds to that calculated by analysis. The employed orientation intensities and the analysis results are shown in Table 8. As shown in the table, the employed orientation intensities for specimen N shows lower values especially for the central section (k=0.2 for layer No.IV), because fibers distribute perpendicularly around specimen center as observed in Section 4.4. In specimens VA and CA, fibers around the central section tend to orient longitudinally. That corresponds to employing higher orientation intensity such as 0.7 for the layer II-IV. In specimen VP, all orientation intensities are 0.4 that is smaller than specimen N, because the fiber orientation to longitudinal direction tends to decrease due to moving the vibrator perpendicular direction. The bending capacity calculated by section analysis can catch the difference of obtained capacity by bending test. The difference can be expressed by the section analysis considering the orientation intensity "k".

Table 8. Analysis condition

Specimen	Orientation intensity of each position of cross-section	Maximum moment(kNm)	
		Test	Analysis
N	I:k=0.6,II:k=0.4,III:k=0.4,IV:k=0.2	7.14	7.17
VA	I:k=0.6,II-IV:k=0.7	8.52	8.65
CA		8.53	8.65
VP	I-IV:k=0.4	7.28	7.22

7 CONCLUTION

1. Placing methods of DFRCC considering fiber orientation using a vibrator and a device like a “comb” are newly proposed. Beam specimens, in which the vibrator or the comb is applied with moving longitudinal direction, show larger bending capacity and ductility.
2. From the results of fracture section observation and flow analysis, the fiber orientation tends to differ in each specimen and in positions of a cross-section.
3. The bending capacity of each specimen is evaluated by section analysis using the bridging law which expresses the difference of fiber orientation for the position of cross-section of the specimen. The difference of bending capacity can be expressed by the section analysis considering the orientation intensity.

8 ACKNOWLEDGEMENT

The authors wish to express their gratitude and sincere appreciation to the Kuraray Co., Ltd. for providing the PVA fiber. This study was supported by the JSPS KAKENHI Grant Number 26289188.

9 REFERENCES

Asano, K. (2014) “Study on Fiber Orientation and Bridging Constitutive Law in High Performance Fiber Reinforced Cementitious Composites”, *Doctoral thesis, University of Tsukuba*, pp.16-31, (in Japanese)

Kanakubo, T., Miyaguchi, M., and Asano, K. (2016) “Influence of Fiber Orientation on Bridging Performance of Polyvinyl Alcohol Fiber-Reinforced Cementitious Composite”, *Materials Journal*, *American Concrete Institute*, Vol.113, No.2, pp.131-141

Kanda, T. and Li, V. C. (1999) “Effect of Fiber Strength and Fiber-Matrix Interface on Crack Bridging in Cement Composites”, *ASCE Journal of Engineering Mechanics*, Vol.125, No.3, pp.290-299